Vol. 68: 185–194, 2013
doi: 10.3354/ame01611

AQUATIC MICROBIAL ECOLOGY
Aquat Microb Ecol

Published online March 18

FEATURE ARTICLE

OPEN ACCESS

Elemental quotas and physiology of a southwestern Pacific Ocean plankton community as a function of iron availability

Steven W. Wilhelm[1,*], Andrew L. King[2], Benjamin S. Twining[3], Gary R. LeCleir[1], Jennifer M. DeBruyn[4], Robert F. Strzepek[5], Cynthia L. Breene[2], Stuart Pickmere[6], Michael J. Ellwood[7], Philip W. Boyd[5], David A. Hutchins[2]

[1]Department of Microbiology, The University of Tennessee, Knoxville, Tennessee 37996, USA
[2]Marine Environmental Biology, Dept of Biological Sciences, University of Southern California, Los Angeles, California 90089, USA
[3]Bigelow Laboratory for Ocean Sciences, PO Box 380, East Boothbay, Maine 04544, USA
[4]Biosystems Engineering and Soil Science, The University of Tennessee, Knoxville, Tennessee 37996, USA
[5]Centre for Chemical and Physical Oceanography, Department of Chemistry, University of Otago, PO Box 56, Dunedin, New Zealand
[6]National Institute of Water and Atmospheric Research, Hamilton 3216, New Zealand
[7]Research School of Earth Sciences, The Australian National University, Canberra, Australian Capital Territory 0200, Australia

ABSTRACT: The rate of carbon fixation by phytoplankton in marine surface waters is often tied to the supply of growth-limiting nutrients such as iron (Fe). While average cellular requirements and ratios for various elements are well known in the literature, especially through laboratory culture work, the plasticity of these relationships in natural plankton communities has been less explored. To gauge how changes in the biological availability of dissolved Fe might influence cellular nutrient ratios of marine phytoplankton (and thus their physiology), we carried out incubation assays during a research expedition off the east coast of New Zealand. Trace-metal clean collection of plankton communities were amended with a continuum of concentrations of either Fe (as $FeCl_3$) or desferroxamine B (to reduce bioavailable Fe) and then maintained for 72 h under *in situ* conditions. Along with standard assays (F_v/F_m, chlorophyll, nutrient drawdown), we measured elemental ratios in the bulk community by inductively coupled plasma mass spectrometry and within individual plankton using synchrotron X-ray fluorescence. Our observations demonstrate that changes in the physiological ecology of the community (biomass, photosynthetic efficiency) were mirrored in changes in elemental ratios, including a 3-fold change in Fe stoichiometry and a 13-fold change in Zn stoichiometry when Fe-replete and Fe-depleted communities were compared. We present this information in consideration of the hypothesis that flexibility in elemental quotas influences the interactions between nutrient availability and planktonic physiological status, subsequently altering C flow through marine surface waters.

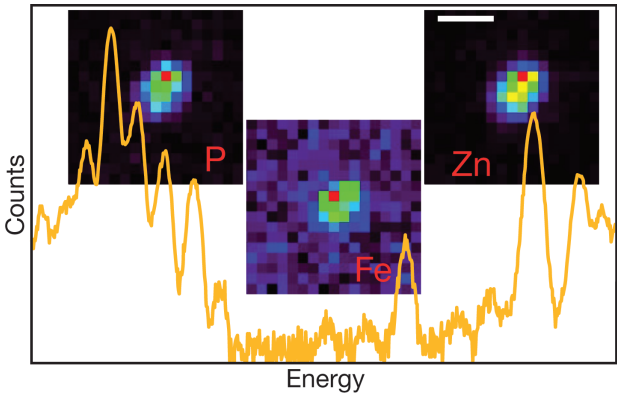

X-ray fluorescence maps of P, Fe and Zn in an autotrophic flagellate overlaid on an X-ray fluorescence spectrum for the cell. Scale bar = 2 µm.

Data collected by: B. S. Twining

KEY WORDS: Cellular iron quotas · Phytoplankton · Marine biogeochemistry

INTRODUCTION

Over the last 25 yr, iron (Fe) has become universally recognized as a key growth-limiting nutrient in many marine ecosystems (reviewed by Hutchins 1995, Wells et al. 1995, Price & Morel 1998, de Baar et

*Email: wilhelm@utk.edu

al. 2005, Boyd et al. 2007). Fe availability governs phytoplankton growth rates and controls community structure throughout the high nutrient–low chlorophyll (HNLC) oceans (de Baar et al. 1990, Martin et al. 1991, Coale et al. 1996, Boyd et al. 2005) as well as in many coastal (Hutchins & Bruland 1998, Hutchins et al. 1998, 2003) and oligotrophic waters (DiTullio et al. 1993, Behrenfeld & Kolber 1999, Behrenfeld et al. 2006). Even though Fe limitation is generally acknowledged to be a critical control of global biological production and organic matter export from surface waters (Sigman & Boyle 2000, Frew et al. 2006), large gaps remain in our understanding of Fe biogeochemistry. Among these is a lack of data on the metabolic plasticity of biogeochemically critical organisms with respect to their cellular Fe usage (Boyd et al. 2007). Indeed, beyond the laboratory culture data sets of Sunda and colleagues (e.g. Sunda & Huntsman 1995), there remains a paucity of quantitative information on the elemental plasticity of marine plankton communities, especially in the natural environment (Twining et al. 2010, 2011, King et al. 2012).

Cellular Fe:C ratios of marine plankton are critical parameters because they directly link the marine biogeochemical cycles of these elements. Fe is now incorporated into many models of marine C biogeochemistry as a consequence of an increased appreciation for the importance of Fe to structure and function of pelagic plankton communities (Lancelot et al. 2000, Fasham et al. 2006, Mongin et al. 2006). In these models, plankton Fe:C ratios often determine the effect of Fe supply on biogeochemical cycling of C and nutrient elements. For example, models linking C and Fe cycles predict that CO_2 drawdown is generally inversely proportional to the assumed Fe:C ratio in plankton cells (Fung et al. 2000). While some models incorporate variability in Fe:C ratios (Moore et al. 2001, 2004, Mongin et al. 2006), very few field data are available with which to compare the model predictions of this parameter.

In laboratory experiments, Fe:C ratios of phytoplankton are considerably plastic, ranging from <1 to >50 µmol mol^{-1} (Sunda & Huntsman 1995, Kustka et al. 2003, Marchetti et al. 2006, Strzepek et al. 2011). For example, the oceanic diatom *Thalassiosira oceanica* can vary its Fe:C ratio from 3 to 30 µmol mol^{-1} without changing its specific growth rate (Sunda et al. 1991). The factors that affect the Fe:C ratios of cyanobacteria and other prokaryotes are less known, but their C- or volume-normalized Fe requirements may be higher than those of many eukaryotic phytoplankton (Brand 1991, Wilhelm 1995, Tortell et al. 1996).

Due to the emphasis by prior research on low-Fe HNLC regions, Fe quotas are particularly unconstrained in Fe-replete locations where luxury uptake may occur and minimum Fe:C ratios cannot be assumed. Bulk particle data from the Atlantic Ocean suggest that phytoplankton Fe quotas may be higher in this ocean basin, which receives significant aeolian Fe input (Helmers 1996, Kuss & Kremling 1999, Tovar-Sanchez et al. 2006, Twining & Baines 2013), but little information is available from high-Fe regimes of the Pacific. In the present study, we manipulated Fe availability in a spring bloom plankton community collected near New Zealand while it was experiencing a transition from Fe-replete to Fe-limited conditions. Using a step-gradient technique involving increasing additions of Fe or the Fe-specific chelator desferroxamine B (DFB) to trace-metal clean microcosms, we generated a continuum of Fe bioavailability resulting in growth conditions within the experiment ranging from Fe-replete to Fe-stressed (cf. Eldridge et al. 2004, 2007). Analyses of individual phytoplankton cells from these Fe-replete and -deplete populations by synchrotron X-ray fluorescence (SXRF) were subsequently compared to bulk measurements of cellular elemental quotas using inductively coupled plasma mass spectrometry (ICP-MS) and to bulk community physiological parameters, to determine how shifts in Fe availability affected the elemental ratios and physiology of this natural spring bloom phytoplankton assemblage.

MATERIALS AND METHODS

Water samples were collected on 3 separate occasions during the occupation of a mesoscale eddy east of New Zealand (Days of Year [DOY] 267, 270, and 275 for Expts 1, 2, and 3, respectively; see Table 1; for further descriptions see Boyd et al. 2012, King et al. 2012). Seawater was directly dispensed into replicate acid-cleaned polycarbonate bottles (2.4 l) for all experiments from a trace-metal clean tow fish system at ~7 m depth utilizing established trace-metal clean techniques (Bowie et al. 2001).

Amendments to bottles generated a range of bioavailable Fe concentrations. Additions of DFB sequestered up to 2.5 nM Fe while additions of $FeCl_3$ increased total Fe up to 2.5 nM above ambient concentrations. DFB additions act to reduce Fe bioavailability by sequestering dissolved Fe in a strong organic ligand complex with very limited bioavailability to most marine plankton (Hutchins et al. 1999, Wells 1999, Eldridge et al. 2004, 2007). Fe and DFB stocks

were made according to the protocol of Eldridge et al. (2004). Control microcosms received no additions. All treatments included independent duplicate microcosms, and results represent the mean and range of duplicate microcosms. Treatments were statistically compared using paired *t*-tests or a 1-way analysis of variance (ANOVA) with Tukey's HSD post hoc means comparison. Treatments were considered significantly different from control if Tukey's HSD test yielded $p < 0.05$.

Microcosms were incubated in a flowing seawater, on-deck shipboard incubator made of Plexiglas™ that attenuated natural sunlight to mimic spectral conditions at a 50% incident irradiance (Wells 1999). Incubations were carried out for 72 h, at which time they were destructively sampled for examination of the parameters listed below. Size-fractionated chlorophyll *a* (chl *a*) concentrations (chl *a* retained on 0.2, 2.0, and 20.0 µm pore size polycarbonate filters) were calculated as the arithmetic mean of measurements from duplicate samples from individual bottles using the non-acidification approach (Welschmeyer 1994). Dissolved nutrients (NO_3, PO_4, SiO_3) were determined by shipboard automated analysis (after Frew et al. 2001), and photosynthetic efficiency (F_v/F_m) values were determined as the mean of 5 repeated measures using fast repetition rate fluorometry as described by McKay et al. (2005).

Community elemental composition

To determine the elemental composition of the community, measurements from the bottle experiments included particulate organic carbon (POC), particulate organic nitrogen (PON), biogenic silica (BSi), particulate Fe (PFe), particulate Al (PAl), particulate Zn (PZn), and particulate P (P) and were determined in Expt 3. All samples were collected with gentle vacuum filtration (<10 mm Hg). For POC/PON, 200 ml aliquots were vacuum-filtered onto pre-combusted 0.7 µm pore-size GF/F filters (Whatman), dried at 60°C, and analyzed via gas chromatography using a CHNS analyzer (Costech). BSi samples (200 ml) were vacuum-filtered onto 0.8 µm pore size polycarbonate filters (Osmonics), dried at 60°C, and analyzed colorimetrically (Leblanc et al. 2005).

Samples for PFe, PAl, PZn, and P analysis by ICP-MS were filtered onto acid-washed (2 M HCl for 1 wk) 47 mm diameter 0.2 µm pore size polycarbonate filter (Poretics) and washed with an oxalate reagent followed by 3 rinses with trace-metal clean filtered seawater to remove extracellular Fe and P (Tovar-Sanchez et al. 2003, Sañudo-Wilhelmy et al. 2004). Each filter was digested with successive additions of 750 µl ultrapure HCl, 250 µl ultrapure HNO_3, and 50 µl ultrapure HF at 100°C for a total of 2 h (all acids from VWR OmniTrace) (Eggimann & Betzer 1976, King et al. 2012). Fe, Al, Zn, and P in the acid-digest solution were analyzed using an Element2 high-resolution ICP-MS (Thermo) (King et al. 2012). Lithogenic Fe (LFe) was calculated using PAl and an Fe:Al molar ratio from an Australian dust sample (mol Fe:mol Al = 0.18; Frew et al. 2006), and is discussed in detail elsewhere (King et al. 2012). Biogenic Fe (BFe) was defined as the difference between PFe and LFe. All sample analyses were blank-corrected for filter, acid, and digestion vessel contributions. Elemental ratios (Fe:P and Zn:P) were determined from oxalate-washed treatments.

Cellular Fe and P concentrations by SXRF analysis

The Fe, Zn, and P contents of individual cells were assessed with SXRF in Expt 3. All SXRF sample processing was conducted in a trace-metal clean van supplied with HEPA-filtered air. All plasticware was acid-washed prior to use, and trace-metal clean techniques were used throughout (Bruland et al. 1979, Twining et al. 2004b). Incubation samples were preserved in glutaraldehyde (0.25% final concentration; trace metal contaminants removed with Dowex resin prior to use) and centrifuged (ca. 3000 × *g*, 30 min) onto 200-mesh gold transmission electron microscopy grids coated with C and Formvar films (Electron Microscopy Sciences). Grids were briefly rinsed in >18.2 M cm^{-1} deionized water and air dried in the dark in a Class-100 laminar-flow hood. The mounted cells were imaged within 24 h using light (Nomarski optics) microscopy and epifluorescence (blue excitation: 480 nm) microscopy.

Elemental quotas for individual cells were measured during a run at the Advanced Photon Source in February 2009 using the hard X-ray microprobe at beamline 2-ID-E following previously described protocols (Twining et al. 2003, 2004a). The cells were analyzed with a monochromatic 10 keV X-ray beam focused to approximately 0.35 µm using a Fresnel zone plate with a 20 cm focal length. Individual cells were scanned in 2-dimensional raster fashion using 0.3 µm step sizes. X-ray fluorescence was collected for 3 s at each pixel to ensure adequate fluorescence photon counts. Forty cells were analyzed in total (14 from control treatment, 10 from +2.5 nM DFB treatment, and 16 from +2.5 nM Fe treatment).

Element quantification of samples from Expt 3 was performed as described by Twining et al. (2011). Briefly, spectra from the pixels representing the target cells were averaged and fit with a custom fitting software package (MAPS; Vogt 2003). Spectra were also averaged for a background region near the cell representing the C/Formvar substrate. Peak areas for the background were subtracted from cellular peak areas. Areal elemental concentrations were calculated for each sample from National Institute of Standards and Technology (NIST) thin-film standard reference materials (NBS 1832 and 1833). Conversion factors for P, S, and Ni (which are not present in the NIST standards) were calculated by interpolation from the conversion factors for Si, K, Ca, Ti, V, Cr, Mn, Fe, Co, Cu, and Zn (Nuñez-Milland et al. 2010).

RESULTS

Station characteristics for sampled water

Stations occupied during this cruise (FeCycle II) were primarily within an eddy located off the northeast coast of New Zealand. Details on the evolution of the spring bloom planktonic community within the gyre are given elsewhere (Boyd et al. 2012, King et al. 2012, Matteson et al. 2012).

Samples collected for the present study were taken early in the cruise (during an *Asterionellopsis glacialis*-dominated bloom; DOY 267, Expt 1), at the midpoint of the cruise (when the bloom was co-dominated by *Synechococcus* spp.; DOY 270, Expt 2), and near the end of the cruise when the phytoplankton community had shifted to *Phaeocystis* (DOY 275, Expt 3). While salinity and temperature remained constant across all 3 sampling times, total chlorophyll was approximately 50% lower during the collection of samples for Expt 3 relative to Expts 1 and 2 (Table 1). In contrast, surface (~7 m) NO_3^- and $Si(OH)_4$ concentrations decreased significantly from samples taken on DOY 267 to those taken on DOY 270, and then returned to near initial concentrations in the water column by Day 275 after the occurrence of a significant wind-induced mixing event on Day 272 (Boyd et al. 2012).

Biomass production, nutrients, and F_v/F_m in experiments

The first experiment initiated on 23 September 2008 (DOY 267) showed no significant effect of either Fe or DFB additions on the phytoplankton community (chlorophyll, nutrient concentrations in experiments, F_v/F_m; data not shown), indicating that the ambient plankton community sampled during the early stages of the bloom was not being constrained by Fe availability (or that cells had large internal Fe stores) and thus we do not consider these results further. In contrast, Expts 2 (DOY 270) and 3 (DOY 275) responded to Fe or DFB additions, indicating that these additions resulted in a physiologically relevant gradient of Fe bioavailability for these communities. Fe additions stimulated chl *a* biomass accumulation in both Expt 2 (Fig. 1A) and Expt 3 (Fig. 1B). In Expt 3, all 3 chl *a* size classes (>0.2, >2.0, >20 µm) were significantly greater in the 0.5, 1.0, and 2.5 Fe addition treatments compared to the control (Tukey, $p < 0.1$; Fig. 1B, Table 2). This stimulation occurred in spite of estimates of dissolved Fe that were similar to concentrations observed during our first experiment (Table 1).

The effects of Fe and DFB on the phytoplankton community physiology were independently confirmed by measurements of F_v/F_m in Expt 2 (Fig. 2A) and Expt 3 (Fig. 2B). In both of these experiments, F_v/F_m values ranged from 0.35 to 0.45 in the DFB treatment, which was significantly lower than the controls (Table 2), to ~0.5 in controls, and 0.57 to 0.6 in the +Fe treatments.

Bulk elemental measurements in Expt 3

In Expt 3, the above observations were linked to apparent biomass production: both particulate N

Table 1. Station locations and initial *in situ* conditions. Where given, variation is the range of duplicate measurements. DOY: Day of Year; SST: sea surface temperature; DRP: dissolved reactive phosphorus

DOY	Latitude (°S)	Longitude (°W)	SST (°C)	Chlorophyll *a* (µg l^{-1}) >0.2 µm	>2.0 µm	>20 µm	Fe (nmol kg^{-1})	Zn	NO_3 (µmol l^{-1})	Si (µmol l^{-1})	DRP (µmol l^{-1})
267 (Expt 1)	39.39	181.31	13.8	1.8 (± 0.1)	1.3 (± 0.1)	0.9 (± <0.1)	0.15	0.04	3.29 (± 0.02)	1.05 (± 0.00)	0.33 (± 0.01)
270 (Expt 2)	39.35	181.15	13.1	1.9 (± <0.1)	1.0 (± 0.1)	0.2 (± <0.1)	0.03	0.05	1.29 (± 0.03)	0.81 (± 0.00)	0.24 (± 0.00)
275 (Expt 3)	39.13	180.83	13.8	0.9 (± <0.1)	0.5 (± <0.1)	0.1 (± <0.1)	0.18	0.17	3.21 (± 0.02)	1.32 (± 0.01)	0.46 (± 0.07)

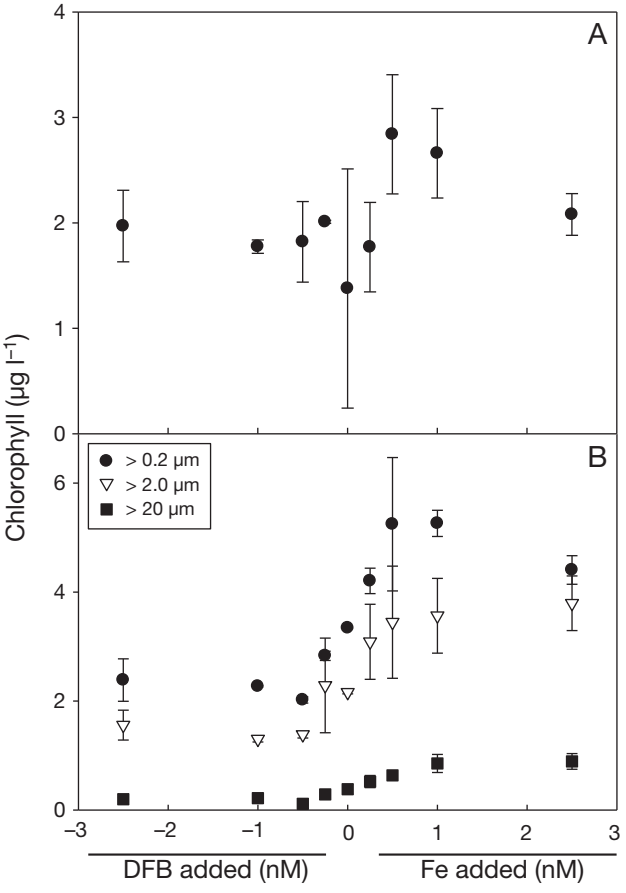

Fig. 1. Phytoplankton biomass production (chlorophyll *a*, ± range, n = 2) in experimental microcosms after the addition of Fe or desferroxamine B (DFB) to samples. Where variation is less than the size of the symbol, error bars are not shown. (A) Total chlorophyll (>0.20 µm) at the termination of Expt 2. No significant differences ($p < 0.05$) were seen in other size classes (not shown). (B) Chlorophyll estimates for >0.20, >2.0, and >20.0 µm size fractions in Expt 3

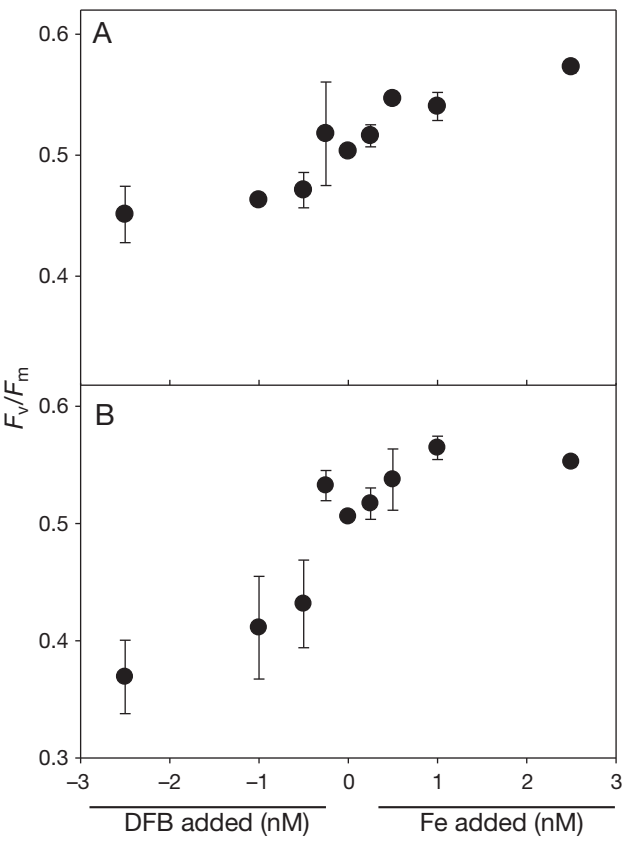

Fig. 2. Photosynthetic efficiency (F_v/F_m) in microcosms after the addition of Fe or desferroxamine B (DFB) to samples. Experimental data shown are for (A) Expt 2 and (B) Expt 3. Where variation is less than the size of the symbol, error bars are not shown

(Fig. 3A) and C (Fig. 3B) appeared higher in +Fe treatments relative to the controls, which in themselves contained more particulate C and N than the +DFB treatments. We note that while treatments were not statistically different from controls in this case (Table 2), the treatments were in some cases statistically different from each other (e.g. for particulate N, +1 nM DFB, and +1 nM Fe, $p = 0.097$; for particulate C, +2.5 nM DFB and +2.5 nM Fe, $p = 0.059$). Incorporation of both of these elements into biomass increased with more Fe, but they did not increase proportionally. C:N ratios in the DFB addition bottles were well below Redfield (~4), but increased progressively with Fe additions up to a maximum of ~5.5 at >1 nM added Fe. Water column particulate Fe:P ratios (estimated by ICP-MS) dropped significantly *in situ* during this period (Table 3). Within the experiments, Fe:P ratios were expectedly higher ($p < 0.05$) in the +Fe treatment relative to the control.

The accumulation of particulate N in biomass resulted in a drawdown of dissolved NO_3^- within Expt 3. Residual nutrient concentrations in the bottles at the termination of this experiment demonstrate that both Si and NO_3^- were significantly altered in the treatments relative to controls ($F = 42$ and 246, $p < 0.001$ for Si and NO_3, respectively): both were depleted in the +Fe bottles, while in the +DFB bottles the drawdown of these nutrients was inhibited and concentrations remained high (Fig. 4, Table 2).

Elemental ratios in individual cells

The Fe quotas of 40 cells (14 control, 10 +DFB, 16 +Fe) from Expt 3 were analyzed with SXRF. All cells

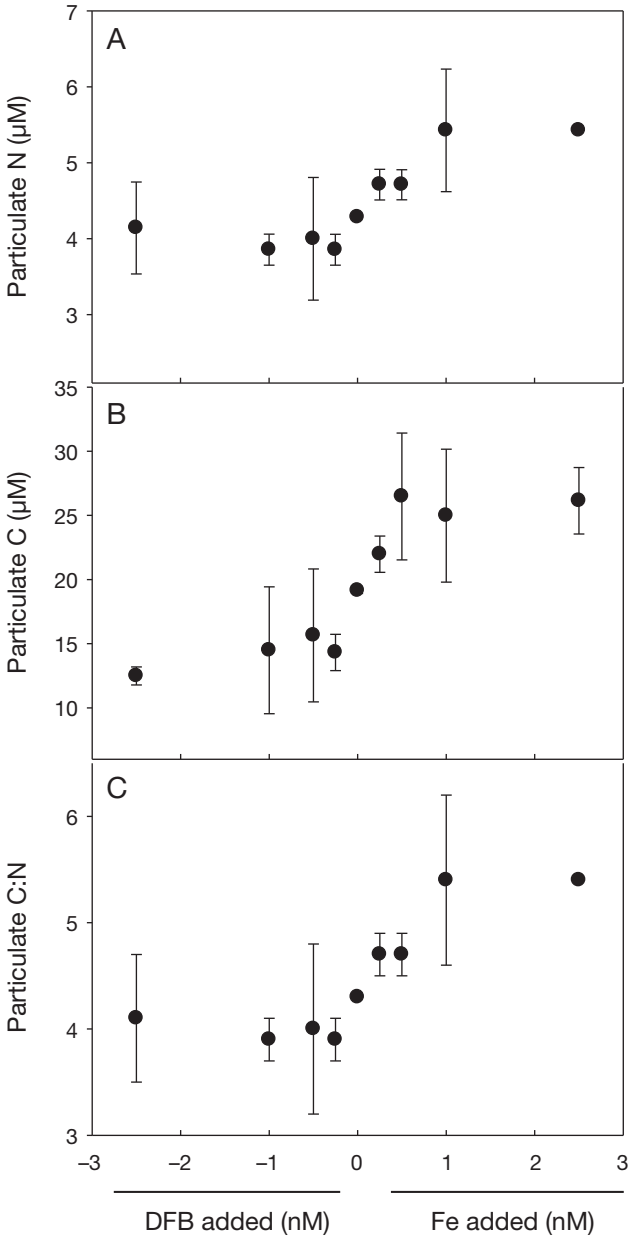

Fig. 3. Particulate (A) nitrogen and (B) carbon from samples collected in Expt 3. Where variation is less than the size of the symbol, error bars are not shown. (C) C:N ratios (molar) from the above data

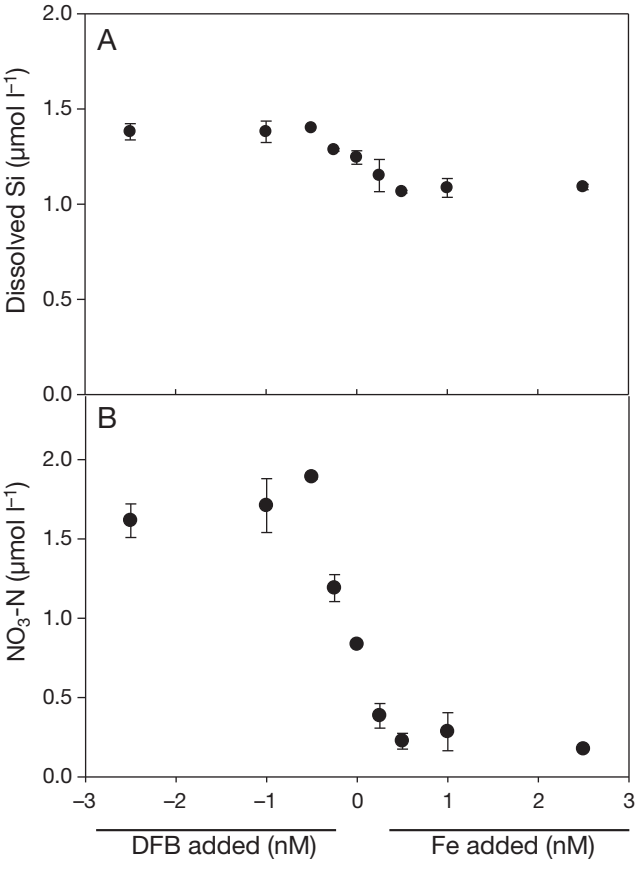

Fig. 4. Dissolved (A) Si and (B) NO_3 concentrations at the termination of Expt 3. Where variation is less than the size of the symbol, error bars are not shown

appeared under light/DIC microscopy as round autotrophs between 1.5 and 2 µm in diameter and were visually consistent with a population of *Phaeocystis* spp. Significant effort was made to choose identical cell types in the 3 treatment bottles; however, little morphological information is available from light microscopy using dry objectives (as required for subsequent SXRF analysis) for cells of this size. Based on the 2D element raster maps (0.3 µm spatial resolution) and biomass quotas of P and S, cells from the +DFB treatment were slightly larger than those from the control and +Fe treatments. Due to the difficulty in confirming that cells from each treatment were from the same taxon, Fe quotas are compared following normalization to the biomass proxy P, which was simultaneously measured with SXRF.

Cellular Fe quotas varied significantly in the treatments as a function of expected Fe availability. The lowest mean Fe quotas (Fe:P = 0.96 mmol mol^{-1}) were observed in cells from the highest DFB addition. Cells in the no-addition control had 2.3-fold higher mean Fe quotas (2.25 mmol mol^{-1}), and cells in the highest Fe addition treatment had 3.1-fold higher mean Fe quotas (2.95 mmol mol^{-1}; Table 3). Treatment differences were deemed significant with pairwise *t*-tests ($p < 0.05$). Interestingly, Zn quotas increased notably (19-fold) in the +Fe treatment compared to the control, but no difference was observed between the control and the +DFB treatment (Table 3).

Table 2. Multiple comparisons of measured variables in Expt 3 microcosms using 1-way ANOVA and Tukey's HSD post hoc means comparison test (α = 0.05). MSE: mean square error; DFB: desferroxamine B; DRSi: dissolved reactive silica; dNO_3: dissolved nitrate

Variable	ANOVA					Tukey's HSD: treatments different from control ('0' treatment) (p < 0.05)	
	MSE treatment	MSE residuals	df	*F*	p	DFB added	Fe added
Particulate N	0.769	0.205	8,9	3.746	0.033	None	None
Particulate C	61.174	12.59	8,9	4.859	0.015	None	None
DRSi	0.076	0.002	8,27	42.023	<0.001	2.5, 1, 0.5	0.5, 1, 2.5
dNO_3	1.928	0.008	8,27	246.05	<0.001	2.5, 1, 0.5, 0.25	0.25, 0.5, 1, 2.5
Chl *a* (>0.2 µm)	6.428	0.204	8,27	31.456	<0.001	0.5	0.5, 1
Chl *a* (>2.0 µm)	3.889	0.344	8,27	11.316	<0.001	None	1, 2.5
Chl *a* (>20 µm)	0.33	0.009	8,27	38.783	<0.001	0.5	0.5, 1, 2.5
F_v/F_m	0.019	0.001	8,27	32.035	<0.001	2.5, 1, 0.5	1

Table 3. Fe:P and Zn:P ratios in control and treatment samples at the termination of Expt 3. Data for *in situ* samples were collected at 30 m with a trace-metal clean rosette (King et al. 2012). Synchrotron X-ray fluorescence (SXRF) data are presented as means ± SE, while inductively coupled plasma mass spectrometry (ICP-MS) data are ±SD of 2 true experimental replicates. ND: not detected; DFB: desferroxamine B

	ICP-MS (mmol:mol)							SXRF (total)	
	Fe:P 0.2–5 µm	Fe:P 0.2–2 µm	Fe:P 2–5 µm	Fe:P 5–20 µm	Fe:P >20 µm	Fe:P total	Zn:P total	Fe: P	Zn:P
In situ									
Day 275 (*T* = 0)	15 ± 10	12 ± 7.0	71 ± 33	18 ± 10	27 ± 33	20 ± 9	3.9 ± 1.3	3.2 ± 1.4[a]	0.36 ± 0.24
Day 278 (*T* = end)	1.6 ± 2.3	1.8 ± 2.7	0.3 ± 0.4	20 ± 18	ND	2.7 ± 2.3	ND	4.8 ± 0.8	1.9 ± 0.51
Treatments									
Control	1.9 ± 0.8	2.0 ± 2.0	1.0 ± 2.3	9.2 ± 11.5	ND	2.5 ± 0.2	2.1 ± 1.7	2.25 ± 0.16	0.69 ± 0.05
+ Fe (2.5 nM)	4.7 ± 0.7	4.7 ± 0.5	4.8 ± 4.7	19.4 ± 10.0	7.0 ± 1.2	7.7 ± 1.5	6.2 ± 2.5	2.95 ± 0.19	13.19 ± 3.54
+ DFB (2.5 nM)	2.8 ± 1.6	2.8 ± 0.6	2.3 ± 4.0	ND	ND	1.9 ± 1.9	3.4 ± 0.8	0.96 ± 0.17	0.95 ± 0.10

[a]Sample for *T* = 0 SXRF taken on Day 273

DISCUSSION

A goal of our incubation experiments was to determine the Fe status of the phytoplankton community during our observations of bloom progression in the eddy. Further considerations were to determine the plasticity of the Fe quotas of the plankton assemblage relative to changing Fe bioavailability, and to examine the resolution of this plasticity with 2 comparable techniques, which we were able to accomplish in Expt 3. The results of this study demonstrate that the spring bloom plankton community during the FeCycle II cruise transitioned from one that was Fe-replete to one that was Fe-limited. Moreover, SXRF and ICP-MS data show that the Fe:P ratios within the community we observed could be readily shifted several fold within a matter of a few days. These results, taken in consideration of our *in situ* observations (King et al. 2012), demonstrate the need to consider elemental plasticity of planktonic communities in both field studies and model simulations.

The 2 elemental analysis methods we employed provide different but complementary data regarding marine planktonic communities. SXRF provides a powerful opportunity to look at the elemental composition of individual plankton morphotypes, while bulk ICP-MS data integrate across the entire planktonic community (including heterotrophic bacteria as well as detrital materials of lithogenic and autochthonous origin). This means that while the bulk ICP-MS data capture community plasticity (including that involved in potential species changes), SXRF can be used to look at species-specific plasticity. For example, *in situ* ICP-MS data demonstrate a marked change in Fe:P in the 2.0 to 5.0 µm size class (from ~71 to 0.3) in just 3 d. While it is possible that significant changes occurred in the elemental quotas of cells in the water column, it is likely that one (or both) of these samples was impacted by non-planktonic materials in a manner that was not accounted for in the Al correction (see King et al. 2012 for more discussion on *in situ* variability). To this end, while both

methods produced results with similar trends in our observations, in reality they likely provide insight into different microbial assemblages.

Previous studies have independently employed Fe addition or sequestration approaches to study community sensitivity to Fe availability (e.g. Hutchins et al. 1999, Maldonado & Price 1999, Wells 1999). Eldridge et al. (2004, 2007) took this approach a step further by combining the use of Fe additions and sequestrations to interpolate the *in situ* conditions of the community (the unamended control). Based on their definitions of cellular Fe status, our results suggest that by DOY 270 to 275, the microbial communities (including algae) were Fe-stressed (i.e. they responded positively to an addition of Fe), but not Fe-starved (i.e. they could be pushed further into Fe-stress by the addition of the DFB chelator).

Within our observations, the most striking results are the plasticity of the elemental quotas within the treatments. By shifting the availability of Fe and driving changes in the physiology of the community (Figs. 1 & 2) and nutrient assimilation (Fig. 3), we were able to demonstrate that cellular metal quotas appear quite plastic. Bulk ICP-MS analyses showed that the Fe:P ratio more than doubled in each size class, with an overall >3-fold increase in Fe:P in the total community sample. In an examination of individual cells using SXRF, the change in Fe:P was less pronounced, but the +Fe treatments still were >30% higher than control cells. In the DFB addition samples, the results are less clear: the lower biomass in these treatments introduced more 'uncertainty' into the data, resulting in large estimates of variance for the size fractions examined by ICP-MS. In examining individual cells by SXRF, however, a decrease to 40% of the control Fe:P was observed in cells. Combining the Fe addition and removal data sets, the results show a 3-fold range in both the total ICPMS Fe:P (from 1.9 to 7.7) and SXRF data (0.96 to 2.95). As noted above, there are several potential reasons for variation in the estimates provided by these 2 techniques, but predominantly the specific targeting of larger cells by SXRF which are likely to be less Fe-rich (relative to other elements) than smaller cells (e.g. *Synechococcus* and heterotrophic bacteria) also included in the ICP-MS data (Wilhelm 1995) may account for this variance in these observations. In total, the results demonstrate that rapid (scale of 1 to 3 d) changes in Fe:P can occur within a community after Fe introduction or removal. Moreover, they demonstrate that a manipulative experiment (as shown in this study) offers the unique opportunity to place *in situ* measurements (cf. King et al. 2012) into the perspective of how carefully controlled changes in Fe availability influence the community. These observations also provide sound corroboration to culture-based studies of marine eukaryotes, where an 8-fold change in cellular Fe quotas was observed (Sunda & Huntsman 1995).

One interesting observation is the significant increase in Zn:P ratios with added Fe. With no obvious explanation at hand, it is quite clear that increasing Fe concentrations within the experiments led to a marked increase in the Zn:P ratio of intact plankton (3-fold comparing control to +Fe for ICMPS data and >13-fold comparing control to treatment for SXRF data). Our initial hypothesis arising from this observation is that alleviation of Fe limitation by the added Fe allowed cells to produce metalloenzymes associated with growth (e.g. carbonic anhydrase: So & Espie 2005; alkaline phosphatase: Twining & Baines 2013) and thus increased their cellular quotas for metals such as Zn. Another possible explanation is that Fe addition may have sufficiently stimulated primary production to the point of CO_2 limitation, resulting in increased carbonic anhydrase production and thus a concurrent increase in Zn:P ratios (Lane & Morel 2000, King et al. 2011). Finally, changes in planktonic community structure may have led to the proliferation of a population with an overall higher Zn:P requirement: parallel *in situ* measurements of particulate (i.e. biological) material collected just after our last experiment demonstrated an increase >5-fold (M. J. Ellwood unpubl.). While the mechanism(s) at hand remain an important topic for future research, the results clearly demonstrate that phytoplankton Fe quotas are not only extremely plastic, but that they can influence cellular requirements for other important trace metals.

Environmental change of any sort is difficult to predict. Marine planktonic communities respond not only to changes in temperature, chemistry, and predation, but do so with a 'metabolic memory' of previous conditions (i.e. the established physiology of the cells, including cellular elemental quotas). As a first step towards making models more dynamic and responsive to environmental change, we must therefore develop an understanding of the plasticity of cellular physiology. This is especially true as it concerns trace elements that can regulate a myriad of cellular processes. The present study demonstrates that large-scale changes in cellular stoichiometry are possible in marine plankton due to small alterations in *in situ* chemistry and that these changes can occur over short (1 to 3 d) time scales. This study sets the foundation for 'flexible quotas' to be included in models of

plankton productivity and climate change, and provides a baseline on how cellular preconditioning (i.e. metabolic memory) influences large-scale biological processes.

Acknowledgements. We thank the captain and crew of the RV 'Tangaroa' as well as all of our colleagues who participated on the cruise, and 2 anonymous reviewers for comments. Work was supported by grants from New Zealand's Coasts and Oceans OBI program (P.W.B.), the Australian Research Council (M.J.E.), and from the US National Science Foundation (OCE 0825379/0825405/0825319 to B.S.T., D.A.H., and S.W.W.). Use of the Advanced Photon Source, an Office of Science User Facility operated for the US Department of Energy (DOE) Office of Science by Argonne National Laboratory, was supported by the US DOE under Contract No. DE-AC02-06CH11357.

LITERATURE CITED

Behrenfeld MJ, Kolber ZS (1999) Widespread iron limitation of phytoplankton in the South Pacific Ocean. Science 283:840–843

Behrenfeld MJ, Worthington K, Sherrell RM, Chavez FP, Strutton P, McPhaden M, Shea DM (2006) Controls on tropical Pacific Ocean productivity revealed through nutrient stress diagnostics. Nature 442:1025–1028

Bowie AR, Maldonado MT, Frew RD, Croot PL and others (2001) The fate of added iron during a mesoscale fertilisation experiment in the Southern Ocean. Deep-Sea Res II 48:2703–2743

Boyd PW, Strzepek R, Takeda S, Jackson G and others (2005) The evolution and termination of an iron-induced mesoscale bloom in the northeast subarctic Pacific. Limnol Oceanogr 50:1872–1886

Boyd PW, Jickells T, Law CS, Blain S and others (2007) Mesoscale iron enrichment experiments 1993–2005: synthesis and future directions. Science 315:612–617

Boyd PW, DeBruyn JM, Ellwood MJ, Hutchins DA and others (2012) Microbial control of diatom bloom dynamics in the open ocean. Geophys Res Lett 39:L18601

Brand LE (1991) Minimum iron requirements of marine phytoplankton and the implications for the biogeochemical control of new production. Limnol Oceanogr 36: 1756–1771

Bruland KW, Franks RP, Knauer GA, Martin JH (1979) Sampling and analytical methods for the determination of copper, cadmium, zinc, and nickel at the nanogram per liter level in sea water. Anal Chim Acta 105: 233–245

Coale KH, Johnson KS, Fitzwater SE, Gordon RM and others (1996) A massive phytoplankton bloom induced by an ecosystem-scale iron fertilization experiment in the equatorial Pacific Ocean. Nature 383:495–501

de Baar HJW, Buma AGJ, Nolting RF, Cadée CG, Jacques G, Tréguer PJ (1990) On iron limitation of the Southern Ocean: experimental observations in the Weddell and Scotia Seas. Mar Ecol Prog Ser 65:105–122

de Baar HJW, Boyd PW, Coale KH, Landry MR and others (2005) Synthesis of iron fertilization experiments: from the Iron Age in the Age of Enlightenment. J Geophys Res 110:C09S16

DiTullio GR, Hutchins DA, Bruland KW (1993) Interaction of iron and major nutrients controls phytoplankton growth and species composition in the tropical North Pacific Ocean. Limnol Oceanogr 38:495–508

Eggimann DW, Betzer PR (1976) Decomposition and analysis of refractory oceanic suspended materials. Anal Chem 48:886–890

Eldridge ML, Trick CG, Alm MB, DiTullio GR and others (2004) Phytoplankton community response to a manipulation of bioavailable iron in HNLC waters of the subtropical Pacific Ocean. Aquat Microb Ecol 35:79–91

Eldridge ML, Cadotte MW, Rozmus AE, Wilhelm SW (2007) The response of bacterial groups to changes in available iron in the eastern subtropical Pacific Ocean. J Exp Mar Biol Ecol 348:11–22

Fasham MJR, Flynn KJ, Pondaven P, Anderson TR, Boyd PW (2006) Development of a robust marine ecosystem model to predict the role of iron in biogeochemical cycles: a comparison of results for iron-replete and iron-limited areas, and the SOIREE iron-enrichment experiment. Deep-Sea Res 53:333–366

Frew R, Bowie A, Croot P, Pickmere S (2001) Macronutrient and trace-metal geochemistry of an in situ iron-induced Southern Ocean bloom. Deep-Sea Res II 48:2467–2481

Frew RD, Hutchins DA, Nodder S, Sañudo-Wilhelmy S and others (2006) Particulate iron dynamics during FeCycle in subantarctic waters southeast of New Zealand. Global Biogeochem Cycles 20:GB1S93

Fung IY, Meyn SK, Tegen I, Doney SC, John JG, Bishop JKB (2000) Iron supply and demand in the upper ocean. Global Biogeochem Cycles 14:281–295

Helmers E (1996) Trace metals in suspended particulate matter of Atlantic Ocean surface water (40° N to 20° S). Mar Chem 53:51–67

Hutchins DA (1995) Iron and the marine phytoplankton community. Prog Phycol Res 11:1–48

Hutchins DA, Bruland KW (1998) Iron-limited diatom growth and Si:N uptake ratios in a coastal upwelling regime. Nature 393:561–564

Hutchins DA, DiTullio GR, Zhang Y, Bruland KW (1998) An iron limitation mosaic in the California upwelling regime. Limnol Oceanogr 43:1037–1054

Hutchins DA, Franck VM, Brzezinski MA, Bruland KW (1999) Inducing phytoplankton iron limitation in iron-replete coastal waters with a strong chelating agent. Limnol Oceanogr 44:1009–1018

Hutchins DA, Pustizzi F, Hare CE, DiTullio GR (2003) A shipboard natural community continuous culture system for ecologically relevant low-level nutrient enrichment experiments. Limnol Oceanogr Methods 1:82–91

King AL, Sañudo-Wilhelmy SA, LeBlanc K, Hutchins DA, Fu F (2011) CO_2 and vitamin B_{12} interactions determine bioactive trace metal requirements of a subarctic Pacific diatom. ISME J 5:1388–1396

King AL, Sañudo-Wilhelmy SA, Boyd PW, Twining BS and others (2012) A comparison of biogenic iron quotas during a diatom spring bloom using multiple approaches. Biogeosciences 9:667–687

Kuss J, Kremling K (1999) Spatial variability of particle associated trace elements in near-surface waters of the North Atlantic (30° N/60° W to 60° N/2° W), derived by large volume sampling. Mar Chem 68:71–86

Kustka AB, Sañudo-Wilhelmy SA, Carpenter EJ, Capone D, Burns J, Sunda WG (2003) Iron requirements for dinitrogen- and ammonium-supported growth in cultures of

Trichodesmium (IMS 101): comparison with nitrogen fixation rates and iron:carbon ratios of field populations. Limnol Oceanogr 48:1869–1884

Lancelot C, Hannon E, Becquevort S, Veth C, De Baar HJW (2000) Modeling phytoplankton blooms and carbon export production in the Southern Ocean: dominant controls by light and iron in the Atlantic sector in Austral spring 1992. Deep-Sea Res I 47:1621–1662

Lane TW, Morel FMM (2000) Regulation of carbonic anhydrase expression by zinc, cobalt, and carbon dioxide in the marine diatom *Thalassiosira weissflogii*. Plant Physiol 123:345–352

Leblanc K, Hare CE, Boyd PW, Bruland KW and others (2005) Fe and Zn effects on the Si cycle and diatom community structure in two contrasting high and low-silicate HNLC areas. Deep-Sea Res I 52:1842–1864

Maldonado MT, Price NM (1999) Utilization of iron bound to strong organic ligands by plankton in the subarctic Pacific Ocean. Deep-Sea Res II 46:2447–2473

Marchetti A, Maldonado MT, Lane ES, Harrison PJ (2006) Iron requirements of the pennate diatom *Pseudo-nitzschia*: comparison of oceanic (high-nitrate, low-chlorophyll waters) and coastal species. Limnol Oceanogr 51: 2092–2101

Martin JH, Gordon RM, Fitzwater SE (1991) The case for iron. Limnol Oceanogr 36:1793–1802

Matteson AR, Loar SN, Pickmere S, DeBruyn JM and others (2012) Production of viruses during a spring phytoplankton bloom in the South Pacific Ocean near New Zealand. FEMS Microbiol Ecol 79:709–719

McKay RML, Wilhelm SW, Hall J, Hutchins DA and others (2005) Impact of phytoplankton on the biogeochemical cycling of iron in subantarctic waters southeast of New Zealand during FeCycle. Global Biogeochem Cycles 19: GB4S24

Mongin M, Nelson DM, Pondaven P, Treguer P (2006) Simulation of upper-ocean biogeochemistry with a flexible-composition phytoplankton model: C, N and Si cycling and Fe limitation in the Southern Ocean. Deep-Sea Res II 53:601–619

Moore JK, Doney SC, Glover DM, Fung IY (2001) Iron cycling and nutrient-limitation patterns in surface waters of the world ocean. Deep-Sea Res II 49:463–507

Moore JK, Doney SC, Lindsay K (2004) Upper ocean ecosystem dynamics and iron cycling in a global 3-dimensional model. Global Biogeochem Cycles 18:GB4028

Nuñez-Milland DR, Baines SB, Vogt S, Twining BS (2010) Quantification of phosphorus in single cells using synchrotron x-ray fluorescence. J Synchrotron Radiat 17: 560–566

Price NM, Morel FMM (1998) Biological cycling of iron in the ocean. In: Sigel A, Sigel H (eds) Iron transport and storage in micro-organisms, plants, and animals, Book 35. Marcel Dekker, New York, NY, p 1–36

Sañudo-Wilhelmy SA, Tovar-Sanchez A, Fu FX, Capone DG, Carpenter EJ, Hutchins DA (2004) The impact of surface-adsorbed phosphorus on phytoplankton Redfield stoichiometry. Nature 432:897–901

Sigman DM, Boyle EA (2000) Glacial/interglacial variations in atmospheric carbon dioxide. Nature 407: 859–869

So AKC, Espie GS (2005) Cyanobacterial carbonic anhydrases. Can J Bot 83:721–734

Strzepek RF, Maldonado MT, Hunter KA, Frew RD, Boyd PW (2011) Adaptive strategies by Southern Ocean phytoplankton to lessen iron limitation: uptake of organically complexed iron and reduced cellular iron requirements. Limnol Oceanogr 56:1983–2002

Sunda WG, Huntsman SA (1995) Iron uptake and growth limitation in oceanic and coastal phytoplankton. Mar Chem 50:189–206

Sunda WG, Swift DG, Huntsman SA (1991) Low iron requirement for growth in oceanic phytoplankton. Nature 351:55–57

Tortell PD, Maldonado MT, Price NM (1996) The role of heterotrophic bacteria in iron-limited ocean ecosystems. Nature 383:330–332

Tovar-Sanchez A, Sañudo-Wilhelmy SA, Garcia-Vargas M, Weaver RS, Popels LC, Hutchins DA (2003) A trace metal clean reagent to remove surface-bound iron from marine phytoplankton. Mar Chem 82:91–99

Tovar-Sanchez A, Sañudo-Wilhelmy SA, Kustka AB, Agusti S and others (2006) Effects of dust deposition and river discharges on trace metal composition of *Trichodesmium* spp. in the tropical and subtropical North Atlantic Ocean. Limnol Oceanogr 51:1755–1761

Twining BS, Baines SB (2013) The trace metal composition of marine phytoplankton. Annu Rev Mar Sci 5:191–215

Twining BS, Baines SB, Fisher NS, Maser J and others (2003) Quantifying trace elements in individual aquatic protist cells with a synchrotron X-ray fluorescence microprobe. Anal Chem 75:3806–3816

Twining BS, Baines SB, Fisher NS (2004a) Element stoichiometries of individual plankton cells collected during the Southern Ocean Iron Experiment (SOFeX). Limnol Oceanogr 49:2115–2128

Twining BS, Baines SB, Fisher NS, Landry MR (2004b) Cellular iron contents of plankton during the Southern Ocean Iron Experiment (SOFeX). Deep-Sea Res I 51: 1827–1850

Twining BS, Nuñez-Milland D, Vogt S, Johnson RS, Sedwick PN (2010) Variations in *Synechococcus* cell quotas of phosphorous, sulfur, manganese, iron, nickel, and zinc within mesoscale eddies in the Sargasso Sea. Limnol Oceanogr 55:492–506

Twining BS, Baines SB, Bozard JB, Vogt S, Walker EA, Nelson DM (2011) Metal quotas of plankton in the equatorial Pacific Ocean. Deep-Sea Res II 58:325–341

Vogt S (2003) MAPS: a set of software tools for analysis and visualization of 3D X-ray fluorescence data sets. J Phys IV 104:635–638

Wells ML (1999) Manipulating iron availability in nearshore waters. Limnol Oceanogr 44:1002–1008

Wells ML, Price NM, Bruland KW (1995) Iron chemistry in seawater and its relationship to phytoplankton — a workshop report. Mar Chem 48:157–182

Welschmeyer NA (1994) Fluorometric analysis of chlorophyll *a* in the presence of chlorophyll *b* and pheopigments. Limnol Oceanogr 39:1985–1992

Wilhelm SW (1995) Ecology of iron-limited cyanobacteria: a review of physiological responses and implications for aquatic systems. Aquat Microb Ecol 9:295–303

Editorial responsibility: Gerhard Herndl, Vienna, Austria

Submitted: September 7, 2012; Accepted: December 19, 2012
Proofs received from author(s): February 10, 2013